AGU PUBLICATIONS

JGR

Journal of Geophysical Research: Space Physics

RESEARCH ARTICLE
10.1002/2016JA023750

Key Points:
- New polar cap patch detection method based on Swarm in situ data provides an unprecedented data set for polar cap patch statistical studies
- Polar cap patch occurrence rate is highest during local winter in both hemispheres; in the south it is also significant during local summer
- There is a clear IMF B_y dependency in the spatial distribution of polar cap patches, consistent with the ionospheric flow pattern

Correspondence to:
A. Spicher,
andres.spicher@fys.uio.no

Citation:
Spicher, A., L. B. N.Clausen, W. J. Miloch, V. Lofstad, Y. Jin, and J. I. Moen (2017), Interhemispheric study of polar cap patch occurrence based on Swarm in situ data, *J. Geophys. Res. Space Physics*, *122*, 3837–3851, doi:10.1002/2016JA023750.

Received 29 NOV 2016
Accepted 6 MAR 2017
Accepted article online 11 MAR 2017
Published online 29 MAR 2017

Interhemispheric study of polar cap patch occurrence based on Swarm in situ data

A. Spicher[1], L. B. N. Clausen[1], W. J. Miloch[1], V. Lofstad[1], Y. Jin[1], and J. I. Moen[1]

[1]Department of Physics, University of Oslo, Oslo, Norway

Abstract The Swarm satellites offer an unprecedented opportunity for improving our knowledge about polar cap patches, which are regarded as the main space weather issue in the polar caps. We present a new robust algorithm that automatically detects polar cap patches using in situ plasma density data from Swarm. For both hemispheres, we compute the spatial and seasonal distributions of the patches identified separately by Swarm A and Swarm B between December 2013 and August 2016. We show a clear seasonal dependency of patch occurrence. In the Northern Hemisphere (NH), patches are essentially a winter phenomenon, as their occurrence rate is enhanced during local winter and very low during local summer. Although not as pronounced as in the NH, the same pattern is seen for the Southern Hemisphere (SH). Furthermore, the rate of polar cap patch detection is generally higher in the SH than in the NH, especially on the dayside at about 77° magnetic latitude. Additionally, we show that in the NH the number of patches is higher in the postnoon and prenoon sectors for interplanetary magnetic field (IMF) $B_y < 0$ and IMF $B_y > 0$, respectively, and that this trend is mirrored in the SH, consistent with the ionospheric flow convection. Overall, our results confirm previous studies in the NH, shed more light regarding the SH, and provide further insight into polar cap patch climatology. Along with this algorithm, we provide a large data set of patches automatically detected with in situ measurements, which opens new horizons in studies of polar cap phenomena.

1. Introduction

Polar cap patches are defined as plasma density enhancements in the *F* region ionosphere at least twice that of the background density [*Crowley*, 1996]. They are islands of plasma which have been cut off from the dayside solar extreme ultraviolet (EUV) produced tongue of ionization by dayside reconnection [e.g., *Knudsen*, 1974; *Foster*, 1984; *Lockwood and Carlson*, 1992; *Sojka et al.*, 1993, 1994; *Carlson et al.*, 2004; *Moen et al.*, 2006; *Clausen and Moen*, 2015]. Subsequently, they are transported by the solar wind-driven polar cap convection through the polar cap, i.e., the region poleward of the auroral oval where the magnetic flux tubes are open with respect to the interplanetary magnetic field (IMF) [e.g., *Brittnacher et al.*, 1999; *Foster et al.*, 2005; *Hosokawa et al.*, 2009a, 2010; *Oksavik et al.*, 2010; *Zhang et al.*, 2013a, 2015]. Patches exit the polar cap into the auroral oval and are called auroral blobs [e.g., *Robinson et al.*, 1985; *Crowley et al.*, 2000; *Lorentzen et al.*, 2004; *Moen et al.*, 2007, 2015; *Jin et al.*, 2014, 2016]. The production of high-density polar cap patches is believed to be predominantly due to transient magnetic reconnection dynamics [e.g., *Lockwood and Carlson*, 1992; *Carlson et al.*, 2004, 2006; *Carlson*, 2012; *Zhang et al.*, 2011, 2013b], which can segment the tongue of ionization into patches by mechanisms including polar cap boundary motions, current sheets, and flow channels [e.g., *Anderson et al.*, 1988; *Lockwood and Carlson*, 1992; *Sojka et al.*, 1993; *Rodger et al.*, 1994; *Valladares et al.*, 1994; *Milan et al.*, 2002; *Pitout and Blelly*, 2003; *Pitout et al.*, 2004; *Carlson et al.*, 2004; *Lockwood et al.*, 2005; *Moen et al.*, 2006; *Carlson*, 2012; *Clausen and Moen*, 2015; *Moen et al.*, 2015].

Polar cap patches are regarded as the main space weather issue in the polar caps as the electron density gradients and irregularities associated with them can disturb HF radio propagation and degrade Global Navigation Satellite Systems signals [e.g., *Spogli et al.*, 2009; *Prikryl et al.*, 2010, 2011; *Moen et al.*, 2013; *Clausen and Moen*, 2015; *Jin et al.*, 2016]. These gradients and irregularities can in particular generate radio wave scintillations, which are rapid fluctuations in the received transionospheric radio wave amplitude and phase [e.g., *Yeh and Liu*, 1982; *Kintner et al.*, 2007]. In order to provide regional forecasts of the scintillations to the user community, it is necessary to precisely identify polar cap patches and improve our knowledge about their dynamics and structuring from the inflow region to their exit from the polar cap. For this, extensive study based on in situ measurements with good coverage over the polar regions is necessary.

Buchau et al. [1983] and *Weber et al.* [1984] undertook pioneering work on polar cap dynamics using all-sky imagers, and since then, numerous other ground-based studies have been carried out, comprising ground-based total electron content (TEC) measurements, incoherent scatter radars, all-sky imagers, and combinations of them [e.g., *Weber et al.*, 1986; *Krankowski et al.*, 2006; *Jin et al.*, 2014, 2016; *Carlson et al.*, 2004; *Oksavik et al.*, 2006; *Moen et al.*, 2006, 2013; *Thomas et al.*, 2015; *Zhang et al.*, 2013a, 2015, 2016a, 2016b; *Hosokawa et al.*, 2006, 2009b, 2016; *Clausen et al.*, 2016].

On the other hand, in situ studies of polar cap patches have progressed slower: Case studies based on rocket or satellite data comprise the works by *Lorentzen et al.* [2010], *Moen et al.* [2012], *Oksavik et al.* [2012], *Spicher et al.* [2014, 2015, 2015b], and *Goodwin et al.* [2015], but comprehensive and statistical studies using in situ measurements are sparse. To date the main contributions for polar cap patch identification based on purely in situ data result from the algorithm developed by *Coley and Heelis* [1995], which allowed to detect and characterize polar cap electron density enhancements using Dynamics Explorer 2 (DE 2) spacecraft density data. This algorithm was then reused by the same authors [*Coley and Heelis*, 1998, 1998a] and by *Kivanç and Heelis* [1997] who studied irregularities associated with patches. Also, using 550 days of DE 2 satellite data, *Burston et al.* [2016] performed a linear growth rate analysis of several instability mechanisms associated with polar cap patches considering the density gradients to be defined as in *Coley and Heelis* [1995].

In addition, *Noja et al.* [2013] recently introduced a new method to detect polar cap patches based on TEC observations aboard CHAMP and presented the patch climatological behavior in both the Northern Hemisphere (NH) and in the Southern Hemisphere (SH). Most of their results for the NH were in agreement with previous results by *Coley and Heelis* [1995] and *Coley and Heelis* [1998a], but compelling differences were observed in the SH, leaving open questions. Indeed, *Coley and Heelis* [1998] found that patch occurrence was maximum during local winter and minimum during local summer in the SH, while *Noja et al.* [2013] found a minimum in local winter and maxima around equinoxes and during local summer.

The methods by *Coley and Heelis* [1995] and *Noja et al.* [2013] have both advantages compared to ground-based techniques, especially for investigating patches in the SH where ground-based instrument studies are challenging. However, they have some limitations: the algorithm by *Coley and Heelis* [1995] does not detect polar cap patches with shallow edges, which can occur, for instance, when the gradient drift instability is extensively acting on the trailing edge of the patch [see, e.g., *Tsunoda*, 1988; *Gondarenko and Guzdar*, 1999; *Spicher et al.*, 2015], while the method by *Noja et al.* [2013] might identify short peaks in TEC values and/or auroral phenomena as polar cap patches.

In order to perform statistical studies of polar cap patches, a robust detection algorithm and extensive data sets are necessary. Unfortunately, such data sets where polar cap patches are automatically identified and which are available to the community are still lacking, even though they are crucial to improve our knowledge about patch dynamics and structuring. For this purpose, we created a new robust algorithm comprising aspects from the two methods above mentioned to automatically detect and flag polar cap patches using in situ plasma density data obtained by the Swarm satellites. The strength of the Swarm satellites was already demonstrated in case studies of patch formation [*Goodwin et al.*, 2015] and patch irregularities [*Spicher et al.*, 2015]: In these studies, they proved that the Swarm satellites were capable of examining polar cap patches.

The outcome of the algorithm, i.e., the data identified as polar cap patches, consists of more than 31 months of data with over 10,000 density enhancements identified as patches in both hemispheres for each of the Swarm satellites (note that the data are daily updated, and thus, the number of polar cap patches detected is increasing as long as the Swarm satellites are operative). It provides an unprecedented data set both for statistical and for case studies of polar cap patches using in situ Swarm measurements and is available to the community at http://www.mn.uio.no/fysikk/english/research/projects/swarm.

In the following, we describe the algorithm in detail, accompanied by a brief comparison with the previous patch detection methods. We then present the seasonal and spatial distributions of the polar cap patches identified by our algorithm between December 2013 and August 2016. We compare and discuss the results with respect to those obtained with other methods.

2. The Polar Cap Patch Detection Algorithm

Launched on 22 November 2013, Swarm is a constellation of the three satellites Alpha (Swarm A), Bravo (Swarm B), and Charlie (Swarm C), whose primary goal is to study the Earth's magnetic field, upper atmosphere,

and ionosphere. After the commissioning phase where the three spacecrafts were flying as pearls on a string in nearly polar circular orbits at an altitude of approximately 500 km, the satellites were maneuvered into their intended main constellation from the middle of January 2014 [e.g., *Lühr et al.*, 2015]; Swarms A and Swarm C are orbiting side by side at about 460 km altitude, while Swarm B orbits at about 510 km altitude. Each satellite has an identical set of instruments [e.g., *Friis-Christensen et al.*, 2006, 2008; *Olsen et al.*, 2013]. Here we present a new algorithm which allows to automatically detect polar cap patches, namely, the Polar Cap Patch Detection Algorithm (PCPDA) using electron density data from the Langmuir probes obtained at a rate of 2 Hz [*Knudsen et al.*, 2014, 2017]. Precisely, the PCPDA reveals whether the density observed by the Swarm satellites is a part of a polar cap patch or not. In the following, the PCPDA is described in detail.

By definition, the plasma density inside a polar cap patch is at least twice that of the surrounding plasma [*Crowley*, 1996]. Thus, polar cap patches can be identified by calculating the ratio inc between the foreground density f and the background density b (inc $= f/b$) in the polar cap. If the ratio inc is greater than 2, the density enhancement with respect to the background agrees with the definition of a patch, whereas if the ratio inc is lower than 2, it does not.

Since, by definition, polar cap patches occur only inside the polar cap, i.e., on open magnetic field lines poleward of the open/closed field line boundary (OCB), the first step in polar cap patch detection is to find the OCB. This is notoriously difficult although many have attempted [*Craven and Frank*, 1987; *Frank and Craven*, 1988; *Lassen and Danielsen*, 1989; *Elphinstone et al.*, 1990; *Mishin*, 1990; *Newell et al.*, 1996; *Germany et al.*, 1997; *Brittnacher et al.*, 1999; *Milan et al.*, 2003; *Wing et al.*, 2010; *Ohtani et al.*, 2010; *Clausen et al.*, 2013]. Here for simplicity, we assume that the OCB is located somewhere below 77° geomagnetic latitude (MLAT), and therefore, we only consider plasma density measurements above that latitude for polar cap patch detection. This is illustrated in Figure 1, where we show the northern polar region using Altitude Adjusted Corrected Geomagnetic Coordinates (AACGM) [*Baker and Wing*, 1989] and the trajectory of Swarm B with the time given in universal time (UT). The pass occurred on 29 December 2013, roughly in the noon-midnight plane. The green region indicates the statistical position of the auroral oval [*Feldstein and Starkov*, 1967] for low geomagnetic activity (*Kp* value of 1) and the thick black circle the 77° MLAT. From Figure 1, it is clear that the statistical oval lies equatorward of the 77° MLAT even for such a low *Kp* value. Thus, it is an adequate choice to assume that the density structures above 77° MLAT are located poleward of the OCB.

After defining the regions where polar cap patches can be detected, a correct identification of the background plasma density inside the polar cap has to be done. This is achieved using a percentile filtering technique, similar to the previous work by *Coley and Heelis* [1995]: in a window of 551 data points, which corresponds to a distance of about 2000 km traveled by the satellite (the sampling frequency being 2 Hz and the velocity of the satellites being about 7.5 km/s), the 35th percentile of the plasma density measurements is calculated; that value is defined as the background plasma density b, and the window is advanced by one data point for the next background calculation. The 35th percentile value was chosen by visual inspection as it provided a good estimate of the background density. Indeed, with this value, large individual density enhancements such as polar cap patches do not affect the determination of the background, and in addition, all plasma density structures with scale size larger than 2000 km are eliminated (the largest extent of polar cap patches is typically 1000 km). Note that the 35th percentile method to calculate the background is significantly better than using the International Reference Ionosphere (IRI) predicted plasma density, as the IRI does not provide data accurate enough within the polar regions.

In order to determine the foreground plasma density f, the original 2 Hz plasma density data provided by the Langmuir probe on board the Swarm satellites are also percentile filtered. As patches are typically several hundreds of kilometers wide [e.g., *Carlson*, 2012], a window of width of seven data points corresponding to a distance of about 25 km in space is chosen for percentile filtering. Within this window the 50th percentile (median) is designated to be the value of the foreground plasma density f, as done in *Coley and Heelis* [1995]. This median filtering process eliminates density features smaller than about 25 km and is chosen so that the fine structures removed are smaller than the typical patch dimension. The foreground f and the background b are then used to calculate the plasma density ratios inc for each satellite pass, and when all values of inc are examined, the algorithm proceeds as follows.

First, the algorithm checks whether the measurement was performed above 77° MLAT (or below −77° MLAT for the SH). If so, the measurement is assumed to be inside the polar cap and the algorithm tests whether inc > 2. If yes, that measurement is considered to be inside of a polar cap patch. Under the condition that

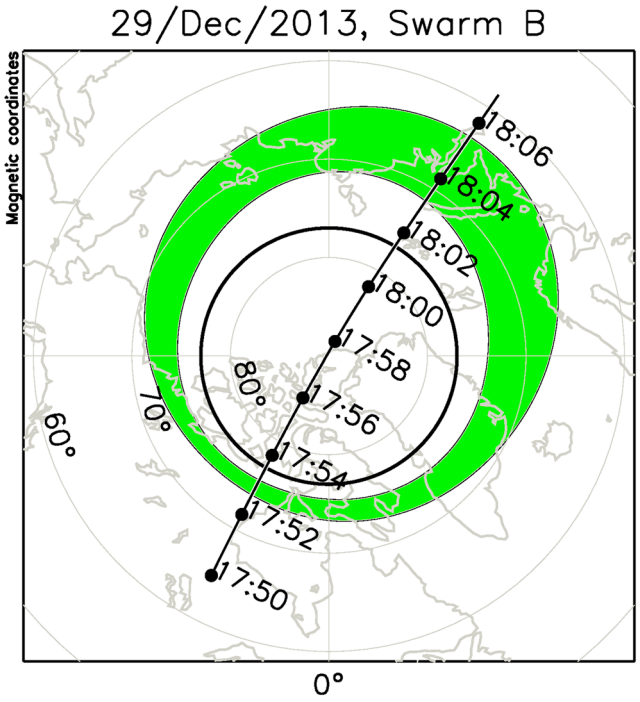

Figure 1. Example of the Swarm B trajectory through the northern polar region in magnetic AACGM coordinates with times in UT. The pass occurred on 29 December 2013. The green region indicates the statistical position of the auroral oval for low geomagnetic activity ($Kp = 1$) and the thick black circle the 77° MLAT.

subsequent inc values also exceed the threshold value of 2, the subsequent density values are also considered to be inside the polar cap patch until inc drops below 2. This region of the plasma density observations, where the foreground is at least twice as large as the background, constitutes what will be called the "patch proper" or PP. Once the PP is identified, the average (mean) background plasma density within the PP, $\overline{PP}$, is calculated. Starting at the beginning of the PP, the algorithm checks whether previous foreground density values drop to within 30% of the $\overline{PP}$ value (i.e., when $f \leq 1.3\ \overline{PP}$). The first value that does so is marked as the beginning of the patch and is referred to as the "first edge." The same procedure is repeated for foreground values following the last value of the PP, and the first value that drops to within 30% of the $\overline{PP}$ marks the end of the patch, i.e., the "second edge." If the entire length of a density enhancement from the beginning of the first edge through the PP to the end of the second edge is longer than 30 data points, which we define as the minimum patch length (with a sampling frequency of 2 Hz, this corresponds to about 100 km), then the density enhancement is identified as a polar cap patch in the Swarm data.

One important point is that during the edge detection process, the foreground plasma density values are compared to the average background of the PP, i.e., $\overline{PP}$, and not to the background b. If the foreground was simply asked to drop to within 30% of the background, steep cliffs would erroneously be identified as polar cap patches. Furthermore, if the foreground does not return to within 30% of $\overline{PP}$ poleward of $|\text{MLAT}| = 75°$, a plasma density enhancement is not identified as a polar cap patch. Note that this allows edges to reach lower latitudes than the threshold of ±77° MLAT of the polar cap.

An example illustrating the detection algorithm for Swarm B is shown in Figure 2: The PP identified is highlighted in gray, the beginning and the end of the edges of the patch are marked by vertical dashed lines, and the horizontal dotted lines mark the average background plasma density inside the PP and its 30% threshold. This patch corresponds to the "dayside" polar cap patch investigated in *Spicher et al.* [2015]. Note that the PCPDA also identified other patches that have been previously discussed in the literature [*Spicher et al.*, 2015; *Goodwin et al.*, 2015]. In addition, we independently tested the PCPDA using all-sky imagers from Svalbard for comparison, which again confirmed that our algorithm adequately detects polar cap patches.

In the past, a few attempts to automatically detect polar cap patches using satellite data have been published. *Coley and Heelis* [1995] used a median filter technique to estimate the background and to filter out small-scale structures. They required that the plasma density enhancements should be at least twice as large as the background density to be qualified as a patch, which is consistent with the definition provided by *Crowley* [1996]. Additionally, they imposed a gradient criterion meaning that the density must increase by at least 40% over the background value over a horizontal distance of 140 km. This algorithm was reused by the same authors [*Coley and Heelis*, 1998, 1998a] and by *Kivanç and Heelis* [1997].

Recently, *Noja et al.* [2013] presented a polar cap patch detection technique based on CHAMP TEC data, which is slightly different: they required the presence of a positive slope in TEC values followed by a negative slope

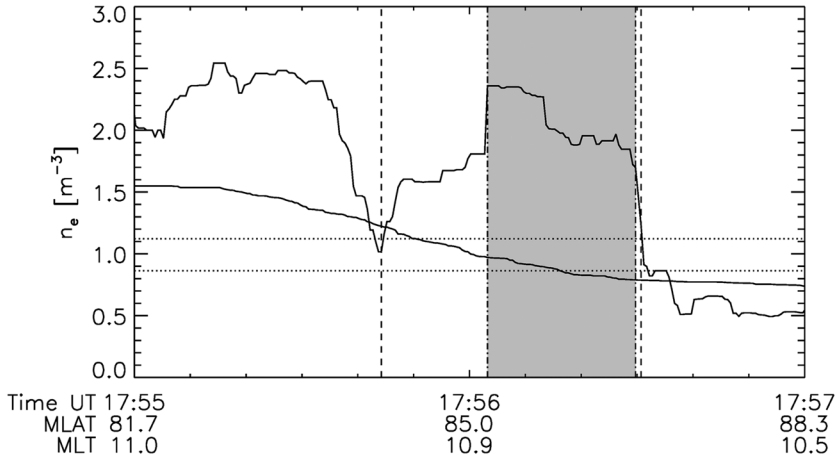

Figure 2. Plasma density data observed by Swarm B (irregular solid line) as well as the corresponding background *b* (smooth solid line). The polar cap patch "proper" (PP) identified by the detection algorithm is highlighted in gray. The beginning and end of the edges are marked by vertical dashed lines, and the horizontal dotted lines mark the average background plasma density inside the PP and the 30% threshold.

within a sliding window, without any restrictions on the size of the slopes. The background plasma density was found by linearly interpolating between the TEC values at the boundaries of the patch range symmetrically to the peak position. If the maximum TEC value between the slopes exceeded a certain threshold with respect to the background, *Noja et al.* [2013] identified the plasma density enhancement as a polar cap patch.

Both these techniques have advantages with respect to ground-based study, but they also have some limitations. By placing a steepness requirement on the slopes, *Coley and Heelis* [1995] could not detect polar cap patches with shallow edges, which is likely to occur on patches where the gradient drift instability is active [e.g., *Spicher et al.*, 2015]. Due to the absence of minimum patch length and constraint on the slopes, sharp peaks in plasma density might be identified as polar cap patches in the method presented in *Noja et al.* [2013]. Furthermore, *Noja et al.* [2013] use a mixture of absolute and relative patch magnitudes as a patch detection criterion, which is different to the generally accepted definition of a polar cap patch as a twofold plasma density increase.

In the PCPDA, we improve these two approaches to detect polar cap patches. As outlined earlier, the objective of the algorithm is to identify and flag plasma density measurements made by the Langmuir probe on board the Swarm satellites which are part of a polar cap patch. Note that an extension to the PCPDA presented here has been developed to provide information whether the edges of the patches are leading or trailing edges, as well as estimates of the linear growth rate of the gradient drift instability. For this, velocity measurements from the Electric Field Instrument on board Swarm [*Knudsen et al.*, 2017] are used in order to determine the direction of motion of polar cap patches relative to that of the satellites. More information about this extension can be found at http://www.mn.uio.no/fysikk/english/research/projects/swarm. In this work, however, we only present the patch detection algorithm which is insensitive to the determination of the leading and trailing edges, and a polar cap patch consists of the first edge, the patch proper and the second edge altogether. Furthermore, our algorithm does not differentiate between approaching density enhancements at different trajectories. One challenge associated with the use of 1-D in situ data only is that a polar cap patch is defined on the basis of the density measurements along the track of the satellite, and the spatial extent of the density enhancement in the other directions remains unknown. On some occasions, this might lead to overdetection or underdetection, and in order to unambiguously address such questions, a combination between ground-based and in situ measurements would be optimal. This is, however, not critical in our polar cap patch climatology study.

In the remainder of the article, we present both the seasonal and spatial distributions of the polar cap patches detected using the PCPDA. By this, we reinvestigate and assess patch climatology results published previously, which is a first step for future polar cap patch studies.

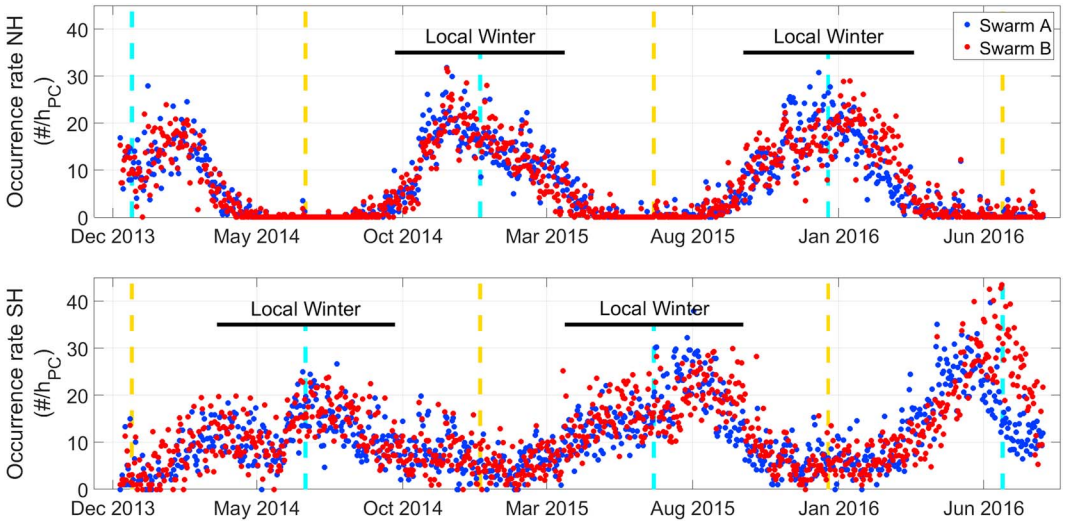

Figure 3. Patch occurrence rate (number of patches normalized by the number of hours, h_{PC}, spent by the satellite in the polar cap above $|MLAT| = 77°$) observed by Swarm A (blue) and Swarm B (red). (top) The Northern Hemisphere (NH) and (bottom) the Southern Hemisphere (SH). The black horizontal lines highlight local wintertime taken between both equinoxes, and the vertical cyan and orange dashed lines mark local winter and summer solstices, respectively.

3. Observations

The data presented here are from 9 December 2013, 00:00:00 UT to 1 August 2016, 23:59:59 UT. The data set comprises more than 10,000 patches detected in each hemisphere for each of the Swarm satellites separately. Due to potential overlaps between the satellites' detections and for comparison purposes, the patch climatology studies are performed individually for each satellite. Since the results obtained from the different satellites generally agree, only observations from Swarm A and B are shown here (Swarm A and Swarm C having similar orbits). The seasonal and spatial distributions of polar cap patches obtained using the PCPDA are given below.

Figure 3 shows the occurrence rate of patches identified per day using the PCPDA for Swarm A (blue) and Swarm B (red) in the Northern Hemisphere (NH) (top) and in the Southern Hemisphere (SH) (bottom). In order to compare both hemispheres, the occurrence rate was calculated as the number of patches observed per day, divided by the time spent by the satellite above $|MLAT| = 77°$ each day. In both hemispheres, the results obtained using Swarm A and Swarm B are very similar during the entire time interval considered.

From Figure 3, it is clear that patch occurrence in the polar cap is seasonally dependent and is enhanced during local winter in both hemispheres. For better visualization, black horizontal lines highlight local wintertime taken between both equinoxes. The vertical cyan and orange dashed lines mark the local winter and summer solstices, respectively. In the NH, most patches are detected during local winter with the largest values being observed around midwinter. In contrast, almost no patches are detected during the local summer months. In the SH, a similar pattern is observed, i.e., an enhanced occurrence in local winter, but the difference between summer and winter is less pronounced and patches are observed throughout all seasons of the year. On average, accounting for all the data points, the occurrence rate is higher in the SH than in the NH by a factor of about 1.5.

In addition to their temporal distribution, the spatial distribution of polar cap patches detected during the same period was computed. For this purpose, a MLAT/magnetic local time (MLT) grid with equal area bins was created for magnetic latitudes ranging from 77° MLAT to 89° MLAT and magnetic local times between 0 MLT and 24 MLT for the NH (−77° MLAT −89° MLAT for the SH). While the latitudinal width of the bins was always 2° MLAT, their longitudinal size was increased from about 20° at $|MLAT| = 77°$ to 120° near the magnetic poles. In each of these bins, the amount of time during which the satellites observed polar cap patches t_p was calculated. Then, to account for orbit effects, the patch observation times t_p were normalized to the amount of time spent by the satellites in each bin t_S, i.e., $P \equiv t_p/t_S$. The ratio P provides a spatial distribution of the patches and can be interpreted as the probability of observing a polar cap patch while being in a bin for our large data set. The results are presented in Figure 4 for Swarm A (Figures 4a and 4c) and Swarm B

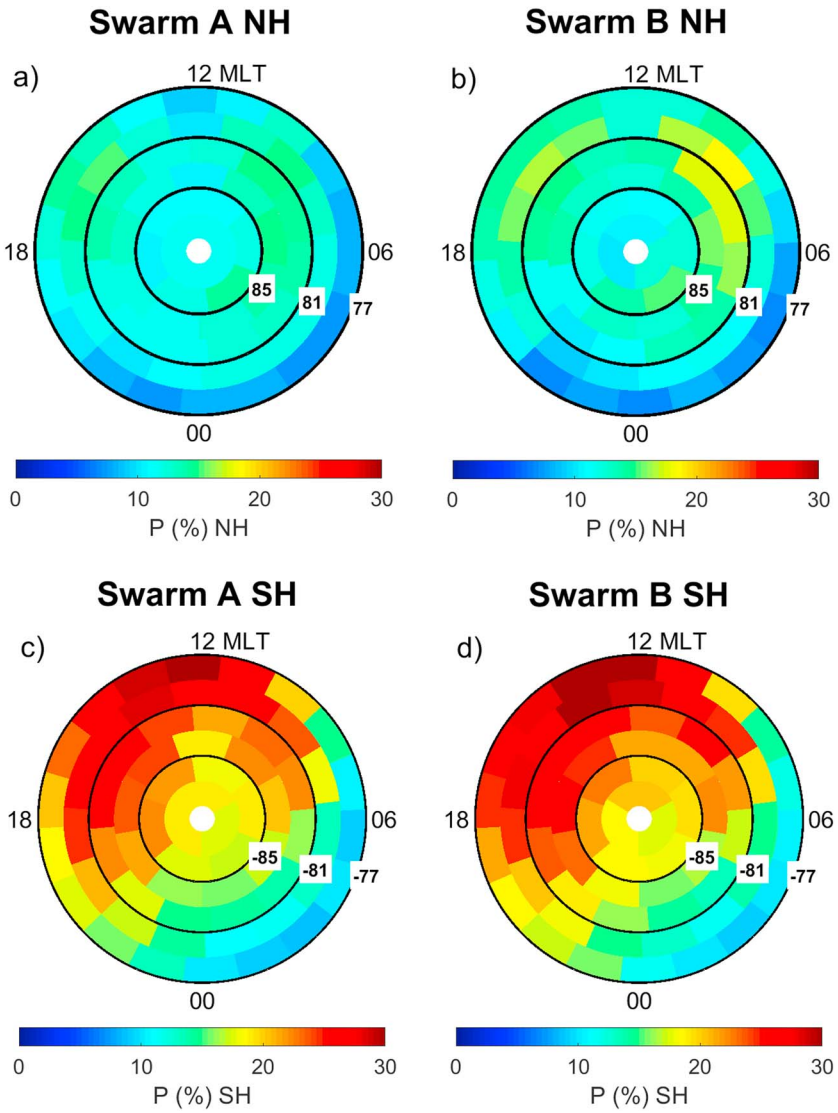

Figure 4. Time duration of patch observations (t_p) in each MLAT/MLT bin normalized by the time spent by the Swarm satellite (t_S) in the respective bin, i.e., $P \equiv t_p/t_S$. Results for (a and c) Swarm A and (b and d) Swarm B. Figures 4a and 4b correspond to the Northern Hemisphere (NH) and Figures 4c and 4d to the Southern Hemisphere (SH).

(Figures 4b and 4d), where Figures 4a and 4b exhibit the time ratio per bin *P* in percent in the NH and Figures 4c and 4d in the SH.

In general, Swarm A and Swarm B observe similar distributions, with a slightly larger occurrence for Swarm B. In the NH, the probability of patch observation is approximately the same at all MLATs and MLTs; i.e., patches are evenly distributed in the polar cap. On average polar cap patches are present 12% (Swarm A) and 13% (Swarm B) of the satellites' observation time. They are detected at minimum about 7% of the time and at maximum about 15% of the time for Swarm A, and the corresponding values are 9% and 19% for Swarm B.

In the SH, polar cap patches are also observed in the entire polar cap, with large values *P* on the dayside, as can be seen in Figure 4. The largest occurrences are concentrated around 12 MLT toward lower magnetic latitudes (below $\approx -81^\circ$ MLAT) with a maximum of about 31% (Swarm A) and 33% (Swarm B), and the distribution is slightly tilted toward dusk. The lowest probabilities of observations are about 9% for both satellites. The mean value of *P* is 19% for Swarm A and 20% for Swarm B for the period considered here, which is about 1.5 times larger than in the NH. This larger occurrence rate in the SH is consistent with the results shown in Figure 3.

As presented in Figure 3, polar cap patches are almost absent during local summer and are enhanced during local winter in the NH, while they can be observed all year round in the SH. Consequently, the spatial

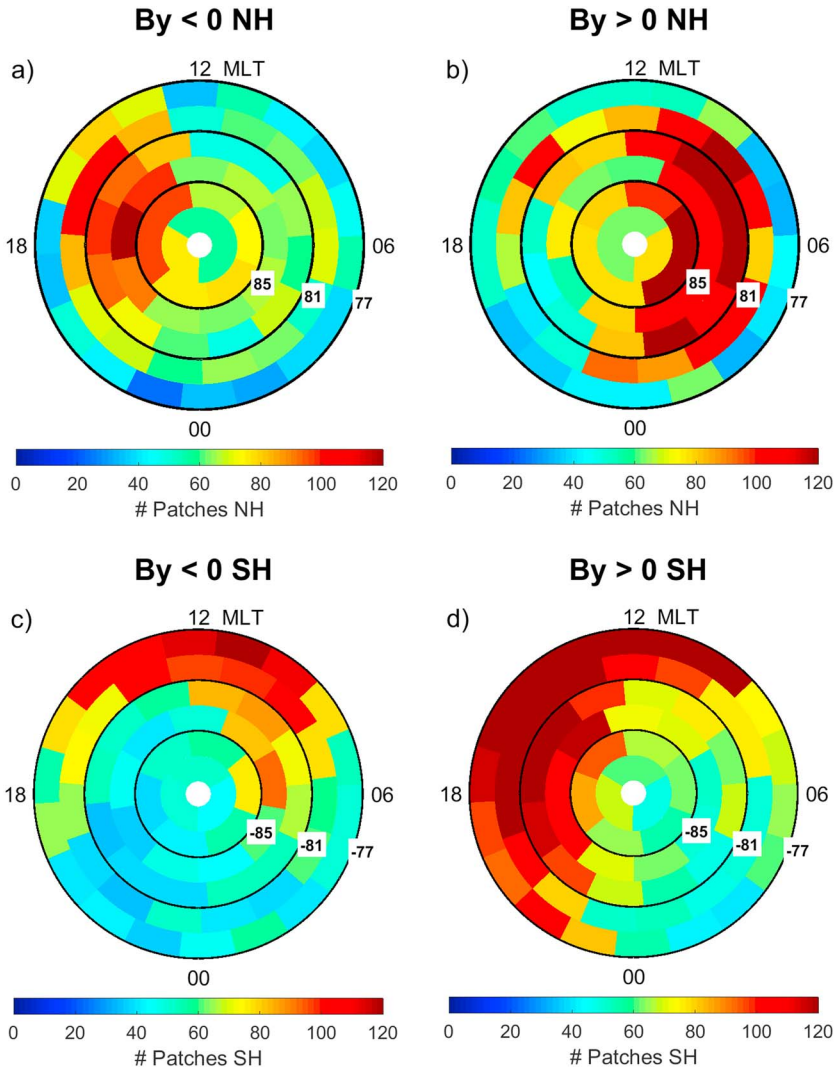

Figure 5. Number of patches detected by Swarm A with respect to 30 min averaged values (a and c) IMF $B_y < 0$ and (b and d) IMF $B_y > 0$. Figures 5a and 5b correspond to the Northern Hemisphere (NH) and Figures 5c and 5d to the Southern Hemisphere (SH).

distributions of polar cap patches shown in Figures 4a and 4b mostly correspond to the local winter spatial distributions in the NH, while in Figures 4c and 4d, they correspond to the distributions observed during the entire years. We also computed the spatial distribution of polar cap patches during equinoxes (March/September) and solstices (December/June) months only (not shown) and retrieved the same seasonal dependency as the one shown in Figure 3. In particular in the NH, the patch ratio per bin P is very low during local summer (June) with a maximum value of ≈2%, while during local summer in the SH (December), P can still reach ≈20% in certain bins (especially at lower latitudes around 12 MLT). During local winter and solstices, patch distributions are more similar in both hemispheres.

Furthermore, we investigated the spatial distribution of polar cap patches with respect to the interplanetary magnetic (IMF) field component B_y, which is believed to influence patch formation, patch trajectory, and structuring [e.g., *Zhang et al.*, 2011; *Moen et al.*, 2015, and references herein]. For this purpose, the median location and observation time of each patch was determined and sorted with respect to the 30 min average of the IMF B_y component preceding the patch observation time. This averaging was chosen in order to be consistent with methods previously published in *Coley and Heelis* [1998a] and *Moen et al.* [2015], and we used the IMF values from the high-resolution OMNI data (1 min) [*King and Papitashvili*, 2005], which monitors the solar wind conditions shifted from the observation point to the bow shock. Then, using the median location of the

polar cap patches, the number of patches observed in each MLAT/MLT equal area bin was calculated for both the averaged IMF values $B_y < 0$ and for the averaged IMF values $B_y > 0$.

The results obtained using the polar cap patches encountered by Swarm A for the same time period as in Figure 4 (Swarm B gave similar results) are presented in Figure 5, which shows the number of patches in each MLAT/MLT bin for IMF $B_y < 0$ (Figures 5a and 5c) and IMF $B_y > 0$ (Figures 5b and 5d) and where Figures 5a and 5b correspond to the NH and Figures 5c and 5d to the SH. As it can be seen in Figures 5a and 5b, sorting the polar cap patch locations with respect to IMF B_y generates a clear dawn-dusk asymmetry in the NH. For IMF $B_y < 0$, the number of polar cap patches is enhanced in the postnoon sectors, with the largest numbers between about 13 MLT and 21 MLT. In contrast, the prenoon sectors between 00 MLT and 12 MLT are strongly favored for IMF $B_y > 0$.

In the SH (see Figures 5c and 5d), the largest number of polar cap patches are observed at lower latitudes around 12 MLT, as already seen in Figure 4, independent of IMF B_y. Additionally, a similar but opposite dawn-dusk asymmetry can be observed in the SH: the number of patches is enhanced in the prenoon sectors for IMF $B_y < 0$, while it is larger in the postnoon sectors for IMF $B_y > 0$.

4. Discussion

In this study, we presented a new algorithm to detect polar cap patches, namely, the PCPDA. Using plasma density measurements made by the Langmuir probes on board the Swarm satellites, we calculated the seasonal and spatial distributions of the polar cap patches detected by the PCPDA. In this section, we review our results with respect to previous studies of polar cap patches.

It is worth mentioning here that it may be possible for a single satellite to detect the same patch more than once and, hence, that we cannot unambiguously assess the total number of different patches detected using the in situ measurements only. For this, when available, support from ground-based instruments which could track single patches would be optimal but impractical for such a big data set. This is, however, not an issue for the patch climatological behavior presented here, as we are not focusing on the distributions of new (different) patches, but mainly on "when" and "where" polar cap patches are detected. As the Swarm satellites cover well the polar regions [e.g., *Stolle et al.*, 2013], as the number of patches detected is very large and as the results from Swarm A and Swarm B agree even though they have different orbits (after the commissioning phase), we estimate that the climatology presented here is well representative of the actual patch distributions in the polar caps.

As presented in Figure 3, the patch occurrence in the polar cap is clearly enhanced during local winter and reduced during local summer in both hemispheres. In the NH, our results agree with previous studies of the seasonal distribution of polar cap patches. Indeed, works by *Coley and Heelis* [1995, 1998, 1998a], who used ion density data from the DE 2 and the DMSP F8 and F9 spacecrafts, and a more recent study from *Noja et al.* [2013], who used TEC data from the CHAMP satellites, showed the same pattern as the one we observe for the NH, that is, a large number of polar cap patches in winter and a very low number in summer in the NH. Also, using digisondes, *Buchau and Reinisch* [1991] showed that in the NH patch-to-background ratios were significantly higher in winter than in summer, with values exceeding 10 and 3 at times, respectively. *Sojka et al.* [1994] and *Wood and Pryse* [2010] performed numerical simulations of patch-to-background ratios and showed that the ratios were much lower in summer. *Wood and Pryse* [2010] observed significant density enhancements in summer, but as their patch-to-background ratios were smaller than 2 in summer, their plasma density enhancements did not meet the definition of a patch. The lack of polar cap patch detection in summer can be explained by the large background electron density maintained in the sunlit polar cap (greater solar EUV production) and thus the difficulty to have persisting high-density enhancements twice as high as the background, as well as by the variation in the chemical composition which both reduces the plasma density drawn into the polar cap and enhances plasma loss by recombination [*Schunk and Sojka*, 1987; *Wood and Pryse*, 2010; *Carlson*, 2012; *Kivanç and Heelis*, 1998]. During summer conditions, solar photoionization smoothes out large-scale structures such as patches which are transported away from their source, meaning that locally produced plasma prevails, while during winter conditions the plasma enhancements transported away from their source dominate in the polar cap [*Kivanç and Heelis*, 1998; *Carlson*, 2012].

In the SH, we observe a similar seasonal pattern as in the NH (see Figure 3), i.e., a general enhancement in patch occurrence during local winter with respect to local summer. This result contrasts the findings by

Noja et al. [2013] who, using TEC data aboard CHAMP from 2001 to 2004, observed relatively large patch occurrence during local summertime and a minimum in June/July, corresponding to local winter in the SH. Note that a local minimum during local winter has also been observed by *Rodger and Graham* [1996], who investigated patch formation pattern in the SH using 2 years of HF radar data from Halley, Antarctica. However, apart from that minimum, *Rodger and Graham* [1996] found a general trend similar to the one we observe, i.e., less patches during local summer compared to local winter. *Noja et al.* [2013] explained their minimum in June/July with the fact that between 2001 and 2004, the TEC was quite inhomogeneous in the SH during local winter months but exhibited very small magnitudes rarely exceeding 5 TECU (total electron content unit, 1 TECU = 10^{16} el m^{-2}) and, hence, that their detection parameters might possibly ignore too small-scale TEC peaks [*Noja et al.*, 2013]. We also observe in the Swarm data that the magnitude of the patch densities and background decrease in the SH during local winter, but polar cap patches can still be detected using the PCPDA. One particular difference between our method and the technique by *Noja et al.* [2013] is that we look for density enhancements in the polar caps only, as we set a threshold to 77° MLAT for patch detection. In *Noja et al.* [2013], this threshold is set to 55° MLAT, which includes cusp and auroral phenomena and might lead to differences. It is also worth mentioning that *Noja et al.* [2013] base their analysis on slant TEC data, which denotes the integrated number of electrons along the line of sight between receiver and transmitter, while we use the electron density observed in situ at the satellite altitudes. Consequently, the exact relationship between the two different techniques is not straightforward.

Overall, our results in the SH agree very well with the in situ study of hemispheric differences in patch occurrence by *Coley and Heelis* [1998], who also detected greater patch numbers in local winter than in local summer in the SH. Moreover, the seasonal dependence we observe matches observations by *Krankowski et al.* [2006], who used GPS TEC fluctuations in the SH and showed that moderate and strong TEC fluctuations of patch activity were maximal from May to September, suggesting that the winter conditions were preferable for patch formation.

In contrast to observations made in the NH where patches are almost completely suppressed in summer, our algorithm detects polar cap patches during the entire year in the SH, reducing the summer/winter difference in occurrence observed in the NH. Again, this coincides well with the results presented in *Coley and Heelis* [1998], where an asymmetry between the NH and SH was also perceptible. Supporting ground-based observations can also be found in *Krankowski et al.* [2006], who showed that patch activity (both strong and low) in the SH was observed the entire year. Furthermore, *Noja et al.* [2013] also observed patches during local summer in the SH and showed that the TEC level was considerable and quite heterogeneous during SH summer, which may explain the detection of polar cap patches. The previous works suggest that this asymmetry in patch occurrence observed in the NH and SH might be a consequence of the magnetic field asymmetry in the NH and SH. Indeed, the offset between the invariant magnetic pole and the geographic poles is larger in the SH than in the NH, and the magnetic flux densities and patterns are different in both hemispheres, which impacts the magnetosphere-ionosphere coupling [e.g., *Förster and Cnossen*, 2013; *Laundal et al.*, 2016] and, by extension, may affect the plasma background and patch distributions as well as patch formation. Assessing these effects is outside the scope of this paper, as numerical simulations are necessary. However, Swarm and the data set presented here provide a great new tool for further interhemispheric studies and for comparison with numerical simulations.

Having discussed the seasonal variations of the polar cap patches detected by the PCPDA, we turn to their spatial distribution. In general, polar cap patches are present at all MLATs and MLTs in the polar cap in both hemispheres. In particular, polar cap patches were found to be present about 13% of the satellites' observation time, averaged over the MLATs and MLTs in the NH, while about 20% in the SH. Thus, the satellites encountered patches in the polar caps about 1.5 more often in the SH than in the NH when orbit effects were taken into consideration. This agrees with the ratios found by *Coley and Heelis* [1998], who detected about twice as many patches in the SH as in the NH and by *Noja et al.* [2013], who saw 60% to 40% more patches in the SH. Again, such difference might be related to the asymmetric magnetic field offset [*Coley and Heelis*, 1998; *Noja et al.*, 2013].

In both the NH and the SH, patches are distributed everywhere, but in addition, there is an enhancement on the dayside in the SH with maximum around noon. This is consistent with *Rodger and Graham* [1996], who found a broad maximum of polar cap patch occurrence centered around magnetic noon in the SH. Essentially, our Figure 4 resembles Figure 4 (top panels) in *Noja et al.* [2013], when considering only latitudes above

|MLAT| = 77° (as our method only focuses on the polar caps). *Noja et al.* [2013] also observed such an enhancement on the dayside SH stretching to magnetic latitudes of about -70^0 with a dusk tail, indicative of the importance of high-density plasma transport from subauroral latitudes on the dayside.

As for the IMF B_y control over the spatial distribution of polar cap patches, we showed the presence of a clear dawn-dusk asymmetry when polar cap patches are sorted with respect to IMF $B_y < 0$ and IMF $B_y > 0$ in the NH. Indeed, for IMF $B_y < 0$ and IMF $B_y > 0$, the number of patches is enhanced in the postnoon and prenoon sectors, respectively. This is in very good agreement with earlier observations [e.g., *Cannon et al.*, 1991; *Fukui et al.*, 1994; *Zhang et al.*, 2003; *Moen et al.*, 2008; *Hosokawa et al.*, 2006; *Yang et al.*, 2016]. The effect of IMF B_y on the trajectory of patch material in the polar caps can be explained by the influence of IMF B_y on the polar ionospheric convection and on poleward moving auroral forms [e.g., *Heppner and Maynard*, 1987; *Zhang et al.*, 2003; *Karlson et al.*, 1996; *Ruohoniemi and Greenwald*, 2005; *Moen et al.*, 2015]. Indeed, for IMF $B_y < 0$, the cusp inflow region is shifted toward prenoon and the patch material will be pulled into the duskside. On the other hand, for IMF $B_y > 0$, the cusp inflow region is shifted toward postnoon and the patches are drawn toward dawnside (see, for example, the scheme in Figure 2 by *Moen et al.* [2008] or Figure 7 by *Jin et al.* [2015]).

In the SH, a mirrored dawn-dusk asymmetry was observed. This can again be explained by the polar ionospheric convection model for which the IMF B_y component has the inverse effect as in the NH [e.g., *Heppner and Maynard*, 1987, and references herein]. Thus, the polar cap patch number is larger on the dawnside for IMF $B_y < 0$ and on the duskside for IMF $B_y > 0$).

In this study, polar cap patches were sorted with respect to the 30 min average of the IMF B_y component preceding the patch observation time, to be consistent with methods previously published in *Coley and Heelis* [1998a] and *Moen et al.* [2015]. In order to include time delays due to the transit times of the patches across the polar regions, precise information on the convection pattern associated with every patch is required and, to be very accurate, a time delay for every patch should be calculated, which is not straightforward. However, using our approximation, we obtain clear results agreeing with previous observations. Note also that shifting this time delay to account for some longer transit time (even for several hours) does not significantly affect the results for our large data set; after computing the autocorrelation function of IMF B_y over the time period investigated here, we suggest that this is due to a long correlation time of the IMF B_y component.

In general, the results obtained using our automatized algorithm confirm previous studies of polar cap patch climatology. We indeed confirm the results obtained by *Coley and Heelis* [1998a] and *Noja et al.* [2013] in the NH. For the SH, our findings regarding the seasonal variations of patches contrast the ones from *Noja et al.* [2013] but corroborate the results by *Coley and Heelis* [1998]. Additionally, by sorting the data by IMF B_y, we confirmed previous studies and, using purely in situ measurements, we provide further evidence of the importance of the B_y in polar cap patch trajectory. Polar cap patches are regarded as the main space weather concern in the polar caps [e.g., *Spogli et al.*, 2009; *Prikryl et al.*, 2010; *Moen et al.*, 2013; *Jin et al.*, 2016], and thus, this work has direct impact for space weather predictions and mitigation.

5. Conclusion

Polar cap patches are regarded as a challenging space weather issue as they are known to degrade HF radio communications and disturb satellite navigation and communication systems. With the increase of human activity in the polar regions relying on such systems, an extensive knowledge about polar cap dynamics and structuring from the inflow region to the exit from the polar cap is of increasing importance.

In this article, we introduced a new algorithm that automatically detects polar cap patches using the in situ plasma density measurements obtained by the Swarm satellites, which offer an outstanding opportunity for polar cap patch studies. Using this algorithm, we presented the spatial and seasonal distributions of the patches identified between 9 December 2013 to 1 August 2016. We showed that both in the Northern Hemisphere (NH) and Southern Hemisphere (SH), the number of polar cap patches is enhanced during local winter, while it is reduced during local summer. Polar cap patches are essentially winter phenomena in the NH, since they are almost totally suppressed during local summer, while they are boosted during local winter. In the SH, patch occurrence is larger during local winter than during local summer, but the difference between the two seasons is not as pronounced as in the NH.

We also showed that the occurrence rate of polar cap patches observed by Swarm is larger in the SH than in the NH. In both hemispheres, patches are observed at all MLATs and MLTs, with an enhancement on the dayside in

the SH. We suggest that the interhemispheric differences result from the interhemispheric asymmetry of the magnetic field, both in strength and in orientation, which impacts the magnetosphere-ionosphere coupling and, by extend, can affect the plasma background and patch distributions, as well as patch formation.

Finally, we showed using purely in situ data that in the NH, the number of patches is enhanced in the postnoon sectors when IMF $B_y < 0$, while it is enhanced in the prenoon sectors when IMF $B_y > 0$ and that this trend is reversed in the SH, consistent with the ionospheric flow convection patterns.

Overall, our results for the NH confirm previous in situ studies by *Coley and Heelis* [1998a] and *Noja et al.* [2013]. Regarding the SH, the seasonal distributions of patches observed by *Noja et al.* [2013] and *Coley and Heelis* [1998a] are contradictory, as *Noja et al.* [2013] observed a minimum in patch occurrence June/July, while *Coley and Heelis* [1998] observed a maximum during local winter. Our results tend to support the findings by *Coley and Heelis* [1998] and provide thus further insight to assess polar cap patch climatology.

Together with the PCPDA, which can be adapted to any spacecraft measuring plasma density, we provide an unprecedented data set of polar cap patches automatically detected in the Swarm data. This opens new doors for statistical and case studies of polar cap patches using in situ measurements which are important for plasma irregularities and scintillations studies in the polar regions and can also provide insights for ionospheric interhemispheric studies.

Acknowledgments
This study was made possible through funding from the European Space Agency (contract 4000114121/15/NL/MP) in the framework of the STSE (Support To Science Element) Swarm+Innovation Program. The list of polar cap patches detected in Swarm data is available through the Polar Cap Product website at http://www.mn.uio.no/fysikk/english/research/projects/swarm. This work was also supported by the Research Council of Norway grant 230996. L.B.N.C. acknowledges funding from the Research Council of Norway under grant 230935. This research is a part of the 4DSpace Strategic Research Initiative at the University of Oslo. The Swarm data can be accessed from ESA at https://earth.esa.int/web/guest/swarm/data-access. The OMNI data were obtained from the GSFC/SPDF OMNIWeb interface at http://omniweb.gsfc.nasa.gov. The authors wish to thank the reviewers for their valuable comments to improve the paper.

References

Anderson, D. N., J. Buchau, and R. A. Heelis (1988), Origin of density enhancements in the winter polar cap ionosphere, *Radio Sci.*, *23*(4), 513–519, doi:10.1029/RS023i004p00513.

Baker, K. B., and S. Wing (1989), A new magnetic coordinate system for conjugate studies at high latitudes, *J. Geophys. Res.*, *94*(A7), 9139–9143, doi:10.1029/JA094iA07p09139.

Brittnacher, M., M. Fillingim, G. Parks, G. Germany, and J. Spann (1999), Polar cap area and boundary motion during substorms, *J. Geophys. Res.*, *104*, 12,251–12,262, doi:10.1029/1998JA900097.

Buchau, J., and B. W. Reinisch (1991), Electron density structures in the polar *F* region, *Adv. Space Res.*, *11*(10), 29–37, doi:10.1016/0273-1177(91)90317-D.

Buchau, J., B. W. Reinisch, E. J. Weber, and J. G. Moore (1983), Structure and dynamics of the winter polar cap *F* region, *Radio Sci.*, *18*(6), 995–1010, doi:10.1029/RS018i006p00995.

Burston, R., C. Mitchell, and I. Astin (2016), Polar cap plasma patch primary linear instability growth rates compared, *J. Geophys. Res. Space Physics*, *121*, 3439–3451, doi:10.1002/2015JA021895.

Cannon, P. S., B. W. Reinisch, J. Buchau, and T. W. Bullett (1991), Response of the polar cap *F* region convection direction to changes in the interplanetary magnetic field: Digisonde measurements in northern Greenland, *J. Geophys. Res.*, *96*(A2), 1239–1250, doi:10.1029/90JA02128.

Carlson, H. C. (2012), Sharpening our thinking about polar cap ionospheric patch morphology, research, and mitigation techniques, *Radio Sci.*, *47*, RS0L21, doi:10.1029/2011RS004946.

Carlson, H. C., K. Oksavik, J. Moen, and T. Pedersen (2004), Ionospheric patch formation: Direct measurements of the origin of a polar cap patch, *Geophys. Res. Lett.*, *31*, L08806, doi:10.1029/2003GL018166.

Carlson, H. C., J. Moen, K. Oksavik, C. P. Nielsen, I. W. McCrea, T. R. Pedersen, and P. Gallop (2006), Direct observations of injection events of subauroral plasma into the polar cap, *Geophys. Res. Lett.*, *33*, L05103, doi:10.1029/2005GL025230.

Clausen, L. B. N., and J. I. Moen (2015), Electron density enhancements in the polar cap during periods of dayside reconnection, *J. Geophys. Res. Space Physics*, *120*, 4452–4464, doi:10.1002/2015JA021188.

Clausen, L. B. N., J. B. H. Baker, J. M. Ruohoniemi, S. E. Milan, J. C. Coxon, S. Wing, S. Ohtani, and B. J. Anderson (2013), Temporal and spatial dynamics of the regions 1 and 2 Birkeland currents during substorms, *J. Geophysical Res. Space Physics*, *118*, 3007–3016, doi:10.1002/jgra.50288.

Clausen, L. B. N., J. I. Moen, K. Hosokawa, and J. M. Holmes (2016), GPS scintillations in the high latitudes during periods of dayside and nightside reconnection, *J. Geophys. Res. Space Physics*, *121*, 3293–3309, doi:10.1002/2015JA022199.

Coley, W. R., and R. A. Heelis (1995), Adaptive identification and characterization of polar ionization patches, *J. Geophys. Res.*, *100*(A12), 23,819–23,827, doi:10.1029/95JA02700.

Coley, W. R., and R. A. Heelis (1998a), Structure and occurrence of polar ionization patches, *J. Geophys. Res.*, *103*(A2), 2201–2208, doi:10.1029/97JA03345.

Coley, W. R., and R. A. Heelis (1998), Seasonal and universal time distribution of patches in the northern and southern polar caps, *J. Geophys. Res.*, *103*(A12), 29,229–29,237, doi:10.1029/1998JA900005.

Craven, J. D., and L. A. Frank (1987), Latitudinal motions of the aurora during substorms, *J. Geophys. Res.*, *92*(A5), 4565–4573, doi:10.1029/JA092iA05p04565.

Crowley, G. (1996), *Critical Review of Ionospheric Patches and Blobs*, edited by W. R. Stone, pp. 619–648, URSI Rev. of Radio Sci. 1993–96996, Oxford.

Crowley, G., A. J. Ridley, D. Deist, S. Wing, D. J. Knipp, B. A. Emery, J. Foster, R. Heelis, M. Hairston, and B. W. Reinisch (2000), Transformation of high-latitude ionospheric *F* region patches into blobs during the March 21, 1990, storm, *J. Geophys. Res.*, *105*(A3), 5215–5230, doi:10.1029/1999JA900357.

Elphinstone, R. D., K. Jankowska, J. S. Murphree, and L. L. Cogger (1990), The configuration of the auroral distribution for interplanetary magnetic field B_z northward: 1. IMF B_x and B_y dependencies as observed by the Viking satellite, *J. Geophys. Res.*, *95*(A5), 5791–5804, doi:10.1029/JA095iA05p05791.

Feldstein, Y., and G. Starkov (1967), Dynamics of auroral belt and polar geomagnetic disturbances, *Planet. Space Sci.*, *15*(2), 209–229, doi:10.1016/0032-0633(67)90190-0.

Foster, J. C. (1984), Ionospheric signatures of magnetospheric convection, *J. Geophys. Res.*, *89*, 855–865, doi:10.1029/JA089iA02p00855.

Foster, J. C., A. J. Coster, P. J. Erickson, J. M. Holt, F. D. Lind, W. Rideout, M. McCready, A. van Eyken, R. J. Barnes, R. A. Greenwald, and F. J. Rich (2005), Multiradar observations of the polar tongue of ionization, *J. Geophys. Res.*, *110*, A09S31, doi:10.1029/2004JA010928.

Frank, L. A., and J. D. Craven (1988), Imaging results from Dynamics Explorer 1, *Rev. Geophys.*, *26*(2), 249–283, doi:10.1029/RG026i002p00249.

Friis-Christensen, E., H. Lühr, and G. Hulot (2006), Swarm: A constellation to study the Earth's magnetic field, *Earth Planets Space*, *58*(4), 351–358, doi:10.1186/BF03351933.

Friis-Christensen, E., H. Lühr, D. Knudsen, and R. Haagmans (2008), Swarm—An Earth observation mission investigating Geospace, *Adv. Space Res.*, *41*, 210–216, doi:10.1016/j.asr.2006.10.008.

Fukui, K., J. Buchau, and C. E. Valladares (1994), Convection of polar cap patches observed at Qaanaaq, Greenland during the winter of 1989–1990, *Radio Sci.*, *29*(1), 231–248, doi:10.1029/93RS01510.

Förster, M., and I. Cnossen (2013), Upper atmosphere differences between northern and southern high latitudes: The role of magnetic field asymmetry, *J. Geophys. Res. Space Physics*, *118*, 5951–5966, doi:10.1002/jgra.50554.

Germany, G. A., G. K. Parks, M. Brittnacher, J. Cumnock, D. Lummerzheim, J. F. Spann, L. Chen, P. G. Richards, and F. J. Rich (1997), Remote determination of auroral energy characteristics during substorm activity, *Geophys. Res. Lett.*, *24*(8), 995–998, doi:10.1029/97GL00864.

Gondarenko, N. A., and P. N. Guzdar (1999), Gradient drift instability in high latitude plasma patches: Ion inertial effects, *Geophys. Res. Lett.*, *26*(22), 3345–3348, doi:10.1029/1999GL003647.

Goodwin, L. V., et al. (2015), Swarm in situ observations of *F* region polar cap patches created by cusp precipitation, *Geophys. Res. Lett.*, *42*, 996–1003, doi:10.1002/2014GL062610.

Heppner, J. P., and N. C. Maynard (1987), Empirical high-latitude electric field models, *J. Geophys. Res.*, *92*(A5), 4467–4489, doi:10.1029/JA092iA05p04467.

Hosokawa, K., K. Shiokawa, Y. Otsuka, A. Nakajima, T. Ogawa, and J. D. Kelly (2006), Estimating drift velocity of polar cap patches with all-sky airglow imager at Resolute Bay, Canada, *Geophys. Res. Lett.*, *33*, L15111, doi:10.1029/2006GL026916.

Hosokawa, K., T. Tsugawa, K. Shiokawa, Y. Otsuka, T. Ogawa, and M. R. Hairston (2009a), Unusually elongated, bright airglow plume in the polar cap *F* region: Is it a tongue of ionization?, *Geophys. Res. Lett.*, *36*, L07103, doi:10.1029/2009GL037512.

Hosokawa, K., T. Kashimoto, S. Suzuki, K. Shiokawa, Y. Otsuka, and T. Ogawa (2009b), Motion of polar cap patches: A statistical study with all-sky airglow imager at Resolute Bay, Canada, *J. Geophys. Res.*, *114*, A04318, doi:10.1029/2008JA014020.

Hosokawa, K., T. Tsugawa, K. Shiokawa, Y. Otsuka, N. Nishitani, T. Ogawa, and M. R. Hairston (2010), Dynamic temporal evolution of polar cap tongue of ionization during magnetic storm, *J. Geophys. Res.*, *115*, A12333, doi:10.1029/2010JA015848.

Hosokawa, K., S. Taguchi, and Y. Ogawa (2016), Periodic creation of polar cap patches from auroral transients in the cusp, *J. Geophys. Res. Space Physics*, *121*, 5639–5652, doi:10.1002/2015JA022221.

Jin, Y., J. I. Moen, and W. J. Miloch (2014), GPS scintillation effects associated with polar cap patches and substorm auroral activity: Direct comparison, *J. Space Weather Space Clim.*, *4*, A23, doi:10.1051/swsc/2014019.

Jin, Y., J. I. Moen, and W. J. Miloch (2015), On the collocation of the cusp aurora and the GPS phase scintillation: A statistical study, *J. Geophys. Res. Space Physics*, *120*, 9176–9191, doi:10.1002/2015JA021449.

Jin, Y., J. I. Moen, W. J. Miloch, L. B. N. Clausen, and K. Oksavik (2016), Statistical study of the GNSS phase scintillation associated with two types of auroral blobs, *J. Geophys. Res. Space Physics*, *121*, 4679–4697, doi:10.1002/2016JA022613.

Karlson, K. A., M. Øieroset, J. Moen, and P. E. Sandholt (1996), A statistical study of flux transfer event signatures in the dayside aurora: The IMF B_y-related prenoon-postnoon symmetry, *J. Geophys. Res.*, *101*(A1), 59–68, doi:10.1029/95JA02590.

King, J. H., and N. E. Papitashvili (2005), Solar wind spatial scales in and comparisons of hourly Wind and ACE plasma and magnetic field data, *J. Geophys. Res.*, *110*, A02104, doi:10.1029/2004JA010649.

Kintner, P. M., B. M. Ledvina, and E. R. de Paula (2007), GPS and ionospheric scintillations, *Space Weather*, *5*, S09003, doi:10.1029/2006SW000260.

Kivanç, Ö, and R. A. Heelis (1997), Structures in ionospheric number density and velocity associated with polar cap ionization patches, *J. Geophys. Res.*, *102*(A1), 307–318, doi:10.1029/96JA03141.

Kivanç, Ö, and R. A. Heelis (1998), Spatial distribution of ionospheric plasma and field structures in the high-latitude *F* region, *J. Geophys. Res.*, *103*(A4), 6955–6968, doi:10.1029/97JA03237.

Knudsen, D., J. Burchill, S. Buchert, I. Coco, L. Toffner-Clausen, and P. E. Holmdahl Olsen (2014), *Swarm Preliminary Plasma Dataset User Note*, pp. 2–12, SWAM-GSEG-EOPG-TN-15-0003, Frascati, Italy.

Knudsen, D. J., J. K. Burchill, S. C. Buchert, A. Eriksson, R. Gill, J.-E. Wahlund, L. Hlen, M. Smith, and B. Moffat (2017), Thermal ion imagers and Langmuir probes in the Swarm electric field instruments, *J. Geophys. Res.*, *122*, 2655–2673, doi:10.1002/2016JA022571.

Knudsen, W. C. (1974), Magnetospheric convection and the high-latitude F_2 ionosphere, *J. Geophys. Res.*, *79*(7), 1046–1055, doi:10.1029/JA079i007p01046.

Krankowski, A., I. Shagimuratov, L. Baran, I. Ephishov, and N. Tepenitzyna (2006), The occurrence of polar cap patches in TEC fluctuations detected using GPS measurements in Southern Hemisphere, *Adv. Space Res.*, *38*(11), 2601–2609, doi:10.1016/j.asr.2005.12.006.

Lassen, K., and C. Danielsen (1989), Distribution of auroral arcs during quiet geomagnetic conditions, *J. Geophys. Res.*, *94*(A3), 2587–2594, doi:10.1029/JA094iA03p02587.

Laundal, K. M., I. Cnossen, S. E. Milan, S. E. Haaland, J. Coxon, N. M. Pedatella, M. Förster, and J. P. Reistad (2016), North–south asymmetries in Earth's magnetic field, *Space Sci. Rev.*, 1–33, doi:10.1007/s11214-016-0273-0.

Lockwood, M., and H. C. Carlson (1992), Production of polar cap electron density patches by transient magnetopause reconnection, *Geophys. Res. Lett.*, *19*(17), 1731–1734, doi:10.1029/92GL01993.

Lockwood, M., J. A. Davies, J. Moen, A. P. van Eyken, K. Oksavik, I. W. McCrea, and M. Lester (2005), Motion of the dayside polar cap boundary during substorm cycles: II. Generation of poleward-moving events and polar cap patches by pulses in the magnetopause reconnection rate, *Ann. Geophys.*, *23*(11), 3513–3532, doi:10.5194/angeo-23-3513-2005.

Lorentzen, D. A., N. Shumilov, and J. Moen (2004), Drifting airglow patches in relation to tail reconnection, *Geophys. Res. Lett.*, *31*, L02806, doi:10.1029/2003GL017785.

Lorentzen, D. A., J. Moen, K. Oksavik, F. Sigernes, Y. Saito, and M. G. Johnsen (2010), In situ measurement of a newly created polar cap patch, *J. Geophys. Res.*, *115*, A12323, doi:10.1029/2010JA015710.

Lühr, H., J. Park, J. W. Gjerloev, J. Rauberg, I. Michaelis, J. M. G. Merayo, and P. Brauer (2015), Field-aligned currents' scale analysis performed with the Swarm constellation, *Geophys. Res. Lett.*, *42*, 1–8, doi:10.1002/2014GL062453.

Milan, S. E., M. Lester, and T. K. Yeoman (2002), HF radar polar patch formation revisited: Summer and winter variations in dayside plasma structuring, *Ann. Geophys.*, *20*(4), 487–499, doi:10.5194/angeo-20-487-2002.

Milan, S. E., M. Lester, S. W. H. Cowley, K. Oksavik, M. Brittnacher, R. A. Greenwald, G. Sofko, and J.-P. Villain (2003), Variations in the polar cap area during two substorm cycles, *Ann. Geophys.*, *21*(5), 1121–1140, doi:10.5194/angeo-21-1121-2003.

Mishin, V. M. (1990), The magnetogram inversion technique and some applications, *Space Sci. Rev.*, *53*(1), 83–163, doi:10.1007/BF00217429.
Moen, J., H. C. Carlson, K. Oksavik, C. P. Nielsen, S. E. Pryse, H. R. Middleton, I. W. McCrea, and P. Gallop (2006), EISCAT observations of plasma patches at sub-auroral cusp latitudes, *Ann. Geophys.*, *24*(9), 2363–2374, doi:10.5194/angeo-24-2363-2006.
Moen, J., N. Gulbrandsen, D. A. Lorentzen, and H. C. Carlson (2007), On the MLT distribution of *F* region polar cap patches at night, *Geophys. Res. Lett.*, *34*, L14113, doi:10.1029/2007GL029632.
Moen, J., X. C. Qiu, H. C. Carlson, R. Fujii, and I. W. McCrea (2008), On the diurnal variability in F_2-region plasma density above the EISCAT svalbard radar, *Ann. Geophys.*, *26*(8), 2427–2433, doi:10.5194/angeo-26-2427-2008.
Moen, J., K. Oksavik, T. Abe, M. Lester, Y. Saito, T. A. Bekkeng, and K. S. Jacobsen (2012), First in situ measurements of HF radar echoing targets, *Geophys. Res. Lett.*, *39*, L07104, doi:10.1029/2012GL051407.
Moen, J., K. Oksavik, L. Alfonsi, Y. Daabakk, V. Romano, and L. Spogli (2013), Space weather challenges of the polar cap ionosphere, *J. Space Weather Space Clim.*, *3*, A02, doi:10.1051/swsc/2013025.
Moen, J., K. Hosokawa, N. Gulbrandsen, and L. B. N. Clausen (2015), On the symmetry of ionospheric polar cap patch exits around magnetic midnight, *J. Geophys. Res. Space Physics*, *120*, 7785–7797, doi:10.1002/2014JA020914.
Newell, P. T., Y. I. Feldstein, Y. I. Galperin, and C.-I. Meng (1996), Morphology of nightside precipitation, *J. Geophys. Res.*, *101*(A5), 10,737–10,748, doi:10.1029/95JA03516.
Noja, M., C. Stolle, J. Park, and H. Lühr (2013), Long-term analysis of ionospheric polar patches based on CHAMP TEC data, *Radio Sci.*, *48*, 289–301, doi:10.1002/rds.20033.
Ohtani, S., S. Wing, P. T. Newell, and T. Higuchi (2010), Locations of night-side precipitation boundaries relative to R2 and R1 currents, *J. Geophys. Res.*, *115*, A10233, doi:10.1029/2010JA015444.
Oksavik, K., J. M. Ruohoniemi, R. A. Greenwald, J. B. H. Baker, J. Moen, H. C. Carlson, T. K. Yeoman, and M. Lester (2006), Observations of isolated polar cap patches by the European Incoherent Scatter (EISCAT) Svalbard and Super Dual Auroral Radar Network (SuperDARN) Finland radars, *J. Geophys. Res.*, *111*, A05310, doi:10.1029/2005JA011400.
Oksavik, K., V. L. Barth, J. Moen, and M. Lester (2010), On the entry and transit of high-density plasma across the polar cap, *J. Geophys. Res.*, *115*, A12308, doi:10.1029/2010JA015817.
Oksavik, K., J. Moen, M. Lester, T. A. Bekkeng, and J. K. Bekkeng (2012), In situ measurements of plasma irregularity growth in the cusp ionosphere, *J. Geophys. Res.*, *117*, A11301, doi:10.1029/2012JA017835.
Olsen, N., et al. (2013), The Swarm Satellite Constellation Application and Research Facility (SCARF) and Swarm data products, *Earth Planets Space*, *65*(11), 1189–1200, doi:10.5047/eps.2013.07.001.
Pitout, F., and P.-L. Blelly (2003), Electron density in the cusp ionosphere: Increase or depletion?, *Geophys. Res. Lett.*, *30*(14), 1726, doi:10.1029/2003GL017151.
Pitout, F., C. P. Escoubet, and E. A. Lucek (2004), Ionospheric plasma density structures associated with magnetopause motion: A case study using the Cluster spacecraft and the EISCAT Svalbard Radar, *Ann. Geophys.*, *22*(7), 2369–2379, doi:10.5194/angeo-22-2369-2004.
Prikryl, P., P. T. Jayachandran, S. C. Mushini, D. Pokhotelov, J. W. MacDougall, E. Donovan, E. Spanswick, and J.-P. St.-Maurice (2010), GPS TEC, scintillation and cycle slips observed at high latitudes during solar minimum, *Ann. Geophys.*, *28*(6), 1307–1316, doi:10.5194/angeo-28-1307-2010.
Prikryl, P., P. T. Jayachandran, S. C. Mushini, and R. Chadwick (2011), Climatology of GPS phase scintillation and HF radar backscatter for the high-latitude ionosphere under solar minimum conditions, *Ann. Geophys.*, *29*, 377–392, doi:10.5194/angeo-29-377-2011.
Robinson, R. M., R. T. Tsunoda, J. F. Vickrey, and L. Guerin (1985), Sources of *F* region ionization enhancements in the nighttime auroral zone, *J. Geophys. Res.*, *90*(A8), 7533–7546, doi:10.1029/JA090iA08p07533.
Rodger, A. S., and A. C. Graham (1996), Diurnal and seasonal occurrence of polar patches, *Ann. Geophys.*, *14*(5), 533–537, doi:10.1007/s00585-996-0533-5.
Rodger, A. S., M. Pinnock, J. R. Dudeney, J. Waterman, O. de la Beaujardiere, and K. B. Baker (1994), Simultaneous two hemisphere observations of the presence of polar patches in the nightside ionosphere, *Ann. Geophys.*, *12*(7), 642–648, doi:10.1007/s00585-994-0642-y.
Ruohoniemi, J. M., and R. A. Greenwald (2005), Dependencies of high-latitude plasma convection: Consideration of interplanetary magnetic field, seasonal, and universal time factors in statistical patterns, *J. Geophys. Res.*, *110*, A09204, doi:10.1029/2004JA010815.
Schunk, R. W., and J. J. Sojka (1987), A theoretical study of the lifetime and transport of large ionospheric density structures, *J. Geophys. Res.*, *92*(A11), 12,343–12,351, doi:10.1029/JA092iA11p12343.
Sojka, J. J., M. D. Bowline, R. W. Schunk, D. T. Decker, C. E. Valladares, R. Sheehan, D. N. Anderson, and R. A. Heelis (1993), Modeling polar cap *F*-region patches using time varying convection, *Geophys. Res. Lett.*, *20*(17), 1783–1786, doi:10.1029/93GL01347.
Sojka, J. J., M. D. Bowline, and R. W. Schunk (1994), Patches in the polar ionosphere: UT and seasonal dependence, *J. Geophys. Res.*, *99*(A8), 14,959–14,970, doi:10.1029/93JA03327.
Spicher, A., W. J. Miloch, and J. I. Moen (2014), Direct evidence of double-slope power spectra in the high-latitude ionospheric plasma, *Geophys. Res. Lett.*, *41*, 1406–1412, doi:10.1002/2014GL059214.
Spicher, A., T. Cameron, E. M. Grono, K. N. Yakymenko, S. C. Buchert, L. B. N. Clausen, D. J. Knudsen, K. A. McWilliams, and J. I. Moen (2015), Observation of polar cap patches and calculation of gradient drift instability growth times: A Swarm case study, *Geophys. Res. Lett.*, *42*, 201–206, doi:10.1002/2014GL062590.
Spicher, A., W. J. Miloch, L. B. N. Clausen, and J. I. Moen (2015b), Plasma turbulence and coherent structures in the polar cap observed by the ICI-2 sounding rocket, *J. Geophys. Res. Space Physics*, *120*, 10,959–10,978, doi:10.1002/2015JA021634.
Spogli, L., L. Alfonsi, G. De Franceschi, V. Romano, M. H. O. Aquino, and A. Dodson (2009), Climatology of GPS ionospheric scintillations over high and mid-latitude European regions, *Ann. Geophys.*, *27*(9), 3429–3437, doi:10.5194/angeo-27-3429-2009.
Stolle, C., R. Floberghagen, H. Lühr, S. Maus, D. J. Knudsen, P. Alken, E. Doornbos, B. Hamilton, A. W. P. Thomson, and P. N. Visser (2013), Space Weather opportunities from the Swarm mission including near real time applications, *Earth Planets Space*, *65*(11), 1375–1383, doi:10.5047/eps.2013.10.002.
Thomas, E. G., et al. (2015), Multi-instrument, high-resolution imaging of polar cap patch transportation, *Radio Sci.*, *50*, 904–915, doi:10.1002/2015RS005672.
Tsunoda, R. T. (1988), High-latitude *F* region irregularities: A review and synthesis, *Rev. Geophys.*, *26*(4), 719–760, doi:10.1029/RG026i004p00719.
Valladares, C. E., S. Basu, J. Buchau, and E. Friis-Christensen (1994), Experimental evidence for the formation and entry of patches into the polar cap, *Radio Sci.*, *29*(1), 167–194, doi:10.1029/93RS01579.
Weber, E. J., J. Buchau, J. G. Moore, J. R. Sharber, R. C. Livingston, J. D. Winningham, and B. W. Reinisch (1984), *F* layer ionization patches in the polar cap, *J. Geophys. Res.*, *89*(A3), 1683–1694, doi:10.1029/JA089iA03p01683.

Weber, E. J., J. A. Klobuchar, J. Buchau, H. C. Carlson, R. C. Livingston, O. de la Beaujardiere, M. McCready, J. G. Moore, and G. J. Bishop (1986), Polar cap *F* layer patches: Structure and dynamics, *J. Geophys. Res.*, *91*, 12,121–12,129, doi:10.1029/JA091iA11p12121.

Wing, S., S.-i. Ohtani, P. T. Newell, T. Higuchi, G. Ueno, and J. M. Weygand (2010), Dayside field-aligned current source regions, *J. Geophys. Res.*, *115*, A12215, doi:10.1029/2010JA015837.

Wood, A. G., and S. E. Pryse (2010), Seasonal influence on polar cap patches in the high-latitude nightside ionosphere, *J. Geophys. Res.*, *115*, A07311, doi:10.1029/2009JA014985.

Yang, S.-G., B.-C. Zhang, H.-X. Fang, Y. Kamide, C.-Y. Li, J.-M. Liu, S.-R. Zhang, R.-Y. Liu, Q.-H. Zhang, and H.-Q. Hu (2016), New evidence of dayside plasma transportation over the polar cap to the prevailing dawn sector in the polar upper atmosphere for solar-maximum winter, *J. Geophys. Res. Space Physics*, *121*, 5626–5638, doi:10.1002/2015JA022171.

Yeh, K. C., and C.-H. Liu (1982), Radio wave scintillations in the ionosphere, *Proc. IEEE*, *70*(4), 324–360, doi:10.1109/PROC.1982.12313.

Zhang, Y., D. J. McEwen, and L. L. Cogger (2003), Interplanetary magnetic field control of polar patch velocity, *J. Geophys. Res.*, *108*(A5), 1214, doi:10.1029/2002JA009742.

Zhang, Q.-H., et al. (2011), On the importance of interplanetary magnetic field B_y on polar cap patch formation, *J. Geophys. Res.*, *116*, A05308, doi:10.1029/2010JA016287.

Zhang, Q.-H., et al. (2013a), Direct observations of the evolution of polar cap ionization patches, *Science*, *339*(6127), 1597–1600, doi:10.1126/science.1231487.

Zhang, Q.-H., B.-C. Zhang, J. Moen, M. Lockwood, I. W. McCrea, H.-G. Yang, H.-Q. Hu, R.-Y. Liu, S.-R. Zhang, and M. Lester (2013b), Polar cap patch segmentation of the tongue of ionization in the morning convection cell, *Geophys. Res. Lett.*, *40*, 2918–2922, doi:10.1002/grl.50616.

Zhang, Q.-H., M. Lockwood, J. C. Foster, S.-R. Zhang, B.-C. Zhang, I. W. McCrea, J. Moen, M. Lester, and J. M. Ruohoniemi (2015), Direct observations of the full Dungey convection cycle in the polar ionosphere for southward interplanetary magnetic field conditions, *J. Geophys. Res. Space Physics*, *120*, 4519–4530, doi:10.1002/2015JA021172.

Zhang, Q.-H., et al. (2016a), Polar cap patch transportation beyond the classic scenario, *J. Geophys. Res. Space Physics*, *121*, 9063–9074, doi:10.1002/2016JA022443.

Zhang, Q.-H., et al. (2016b), Earth's ion upflow associated with polar cap patches: Global and in situ observations, *Geophys. Res. Lett.*, *43*, 1845–1853, doi:10.1002/2016GL067897.